Performance Characterization of a High-Power Dual Active Bridge dc-to-dc Converter

Mustansir H. Kheraluwala, Randal W. Gascoigne, *Member, IEEE*, Deepakraj M. Divan, *Member, IEEE*, and Eric D. Baumann

Abstract—**This paper describes the performance of a high-power, high-power-density dc-to-dc converter based on the single-phase dual active bridge (DAB) topology [1]. The dual active bridge converter was shown to have very attractive features in terms of low device and component stresses, small filter components, low switching losses (by virtue of zero voltage switching), high-power density and high efficiency, bidirectional power flow, buck-boost operation, and low sensitivity to system parasitics. For high-output voltages, in the order of kilovolts, a cascaded output structure is considered. The impact of snubber capacitance and magnetizing inductance on the soft switching region of control are discussed. Various control schemes are outlined. Since the leakage inductance of the transformer is used as the main energy transfer element, coaxial transformer design techniques [2] have been utilized to carefully control this parameter. The actual layout and experimental performance of a prototype 50-kW, 50-kHz unit operating with an input voltage of 200 Vdc and an output voltage of 1600 Vdc is presented.**

Introduction

THE FIELD OF HIGH-power-density dc-to-dc converters has received a lot of attention in recent years. In particular, for low-power converters, there has been a proliferation of resonant, quasiresonant, multiresonant, and resonant-transition converters that offer the advantages of soft switching and high switching frequencies [3–6]. By way of contrast, very little has been done in the area of high-power dc-to-dc converters that are subject to similar power density constraints. Schwarz was the first to explicitly recognize the benefits of resonant switching for the realization of dc-to-dc converters rated in the tens of kilowatts [7]. Although series and parallel resonant converters have since been applied in x-ray, welding, and traction applications, resonant converters in high-power applications demand a significant penalty in terms of device and component VA stresses. As a result, hard-switching pulse-width-modulated dc-to-dc converters have been the topology of choice in the past.

A more attractive approach for higher power levels is the family of resonant-transition or pseudo-resonant converters. These converters have been demonstrated to have very moderate component ratings and low switching loss. The dual active bridge (DAB) converter, which is proposed in [1], has been shown to be an attractive alternative for high-power applicaitons. The converter uses active devices on both the input and output sides to realize a minimal topology that has low device stresses, no extra reactive components, and uses the transformer leakage inductance as the main energy transfer element. The ripple current levels in the input and output filter capacitors are also seen to be reasonable. The topology also permits high-frequency operation as a result of zero voltage switching for all the devices over a reasonable operating range. The DAB converter is also seen to be the dual of a converter proposed by Mohan and Peterson for superconducting magnetic energy storage systems (SMES) and has also been referred to as the inductor-converter bridge (ICB) [8], [9]. The use of thyristors in the ICB, in particular, in a hard switching environment, restricts the maximum frequency attainable. Further, the need for transformer isolation would cause serious problems due to the energy trapped in the leakage inductance. Consequently, the DAB topology is considered to be more attractive, especially where power density is important.

This paper presents the performance characteristics of a high-power DAB dc-to-dc converter for aerospace applications. The converter has been designed with power density as the primary objective. The converter is rated at 50 kW with an input of 200 V and an output of 1600 V and is aimed at establishing a modular concept for high-voltage output supplies. The unique combination of high-frequency, high-output-voltage and an active output bridge can only be met with a series-connected output structure. This paper presents a brief analysis of the topology including parasitic and snubber effects, control techniques for bidirectional power flow using voltage or current mode controllers, and experimental results verifying operation of the converter. Power density figures attained with this converter are also presented.

Paper IPCSD 91-80, approved by the Industrial Power Conversion Committee of the IEEE Industry Applications Society for presentation at the 1990 Industry Applications Society Annual Meeting, Seattle, WA, October 7–12. This work was supported by a research grant from the NASA Lewis Research Center, Cleveland, OH. Manuscript released for publication May 10, 1991.

M. H. Kheraluwala and R. W. Gascoigne are with Corporate Research and Development, General Electric Company, Schenectady, NY 12301.

D. M. Divan is with the Department of Electrical and Computer Engineering, University of Wisconsin, Madison, WI 53706-1691.

E. D. Baumann is with the NASA Lewis Research Center, Cleveland, OH 44135.

IEEE Log Number 9203297.

0093-9994/92$03.00 © 1992 IEEE

BACKGROUND

Fig. 1(a) shows the circuit schematic of the single-phase DAB dc-to-dc converter [1], [10], [11]. The principle of operation of the DAB dc-to-dc converter is very simple. Two active bridges are interfaced through a transformer and are phase shifted from each other to control the amount of power flow from one dc voltage source to the other. This allows a fixed frequency, square-wave mode of operation and utilization of the leakage inductance of the transformer as the main energy transfer element. Fig. 1(b) shows the simulated operating waveforms. The output power under idealized conditions is derived as

$$P_o = \frac{V_i^2}{X_L} d\phi\left(1 - \frac{|\phi|}{\pi}\right) \tag{1}$$

where

$$X_L = \omega L, \quad d = \frac{V_o}{NV_i}$$

and V_i is the input dc voltage, V_o is the output dc voltage, ω is the switching frequency in radians per second, L is the primary-referred leakage inductance, N is the transformer turns ratio, and ϕ is the phase shift between the input and output bridges. Fig. 2 shows the family of output power versus phase-shift curves with d as the parameter for both forward and reverse power flow. During forward power flow, the source side bridge leads the load side bridge, designated as positive phase-shifts; in the reverse mode, the load side bridge leads the source side bridge. The region of soft switching for all the devices is identified. Full control range under soft switching is achievable for $d = 1$ and, hence, is usually chosen as a convenient design point. For buck ($d < 1$) or boost ($d > 1$) operation, the control range is reduced under soft-switching conditions in both the quadrants.

For the power supply designer, a more useful piece of information is the output voltage versus output current characteristic for the converter. This information is presented as a nomogram in Fig. 3. The bold curves enclose the region of operation of the DAB converter under soft-switching conditions. Full control under soft switching is achievable at $d = 1$. Under lightly loaded conditions, as $R \to \infty$, the soft-switching region decreases. The intersection of the constant d lines and the constant R lines (load lines) gives the operating phase shift, ϕ. Similarly, the intersection of the constant ϕ lines and the constant R lines indicates an operating d for the converter. Such a nomogram is very useful in ascertaining, rather quickly, if an operating point is within the soft-switching region or not.

The above analysis has been carried out under the assumptions that the transformer magnetizing inductance is infinite and the device snubber capacitances are negligible. The following sections study the influence of these parameters on the soft-switching region of operation for the dual active bridge dc-to-dc converter.

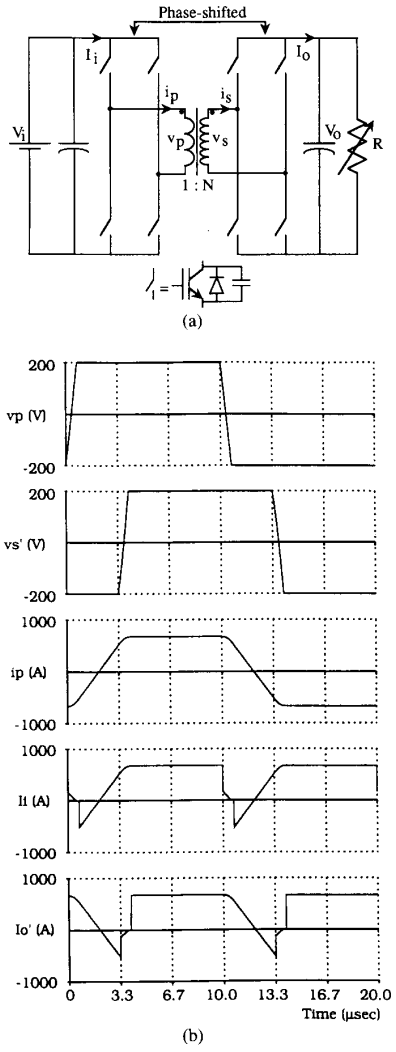

Fig. 1. (a) Circuit schematic of single phase dual active bridge dc-to-dc converter; (b) computer simulated DAB converter waveforms. Operating point is $d = 1$, $\phi = 60°$. The IGBT turn-off switching model of [10] is assumed.

INFLUENCE OF DOMINANT SYSTEM PARASITICS ON SOFT-SWITCHING OPERATION

Transformer Magnetizing Inductance

This section analyzes the influence of the transformer magnetizing inductance on the soft-switching region of operation of the DAB converter. Fig. 4 shows the primary referred model for the converter, with the input and output bridges replaced by square wave voltage sources. The T model has been assumed for the transformer, with the leakage inductance split equally on each side of the finite magnetizing inductance. It is valid to assume that the winding resistances are negligible compared with the leakage reactance at the high frequencies of interest. Let the magnetizing inductance $L_m = K^*L$, where L is the total leakage inductance and $K \geq 1$. The currents i_p and

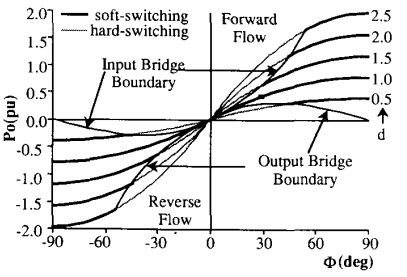

Fig. 2. Family of output power versus phase-shift, with d as a parameter. The bidirectional power flow characteristics are shown.

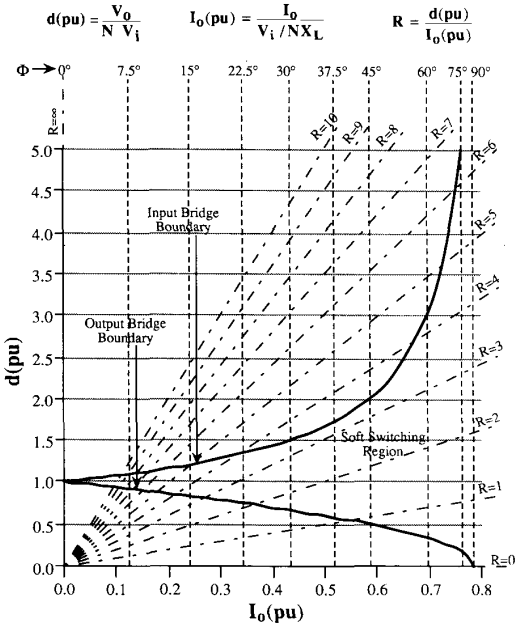

Fig. 3. Nomogram of output voltage versus output current. R is the normalized load resistance.

i'_s are expressed as

$$\frac{di_p}{d\theta} = K_1 v_p - K_2 v'_s \tag{2}$$

$$\frac{di'_{s1}}{d\theta} = K_2 v_p - K_1 v'_s \tag{3}$$

where

$$K_1 = \frac{1 + \dfrac{1}{2K}}{X_L\left(1 + \dfrac{1}{4K}\right)} \tag{4a}$$

and

$$K_2 = \frac{1}{X_L\left(1 + \dfrac{1}{4K}\right)} \tag{4b}$$

and $\theta = \omega t$.

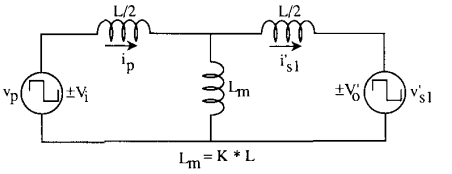

Fig. 4. Primary-referred T model of the transformer. The input and output bridges are replaced by equivalent square-wave voltage sources.

Solving for the currents and enforcing the zero-voltage switching constraints, we arrive at the following control inequalities. For the input bridge

$$d \le \frac{K_1}{K_2}\left[\frac{\pi}{\pi - 2\phi}\right] \qquad 0 \le \phi \le \frac{\pi}{2} \tag{5a}$$

and for the output bridge

$$d \ge \frac{K_2}{K_1}\left[1 - \frac{2\phi}{\pi}\right] \qquad 0 \le \phi \le \frac{\pi}{2}. \tag{5b}$$

The average output current, I'_o normalized to V_i/X_L is

$$I'_o = K_2 X_L \phi\left[1 - \frac{\phi}{\pi}\right]. \tag{6}$$

To illustrate the influence of the magnetizing inductance, the soft-switching region of the converter is depicted on the output voltage versus output current plane for two values of K, as shown in Fig. 5, using 5(a), 5(b), and 6. The selected values for K represent either extreme for the magnetizing inductance. As seen for low values of the output current, the region of soft switching widens as K decreases. This is seen to be reasonable because with decreasing magnetizing inductance, the load appears more lagging, which is a precondition for zero-voltage switching. The penalty for lower magnetizing inductance is low transformer utilization. This result can be used to advantage for applications requiring efficient voltage control at lightly loaded conditions. In addition, the maximum average output current, which is governed by the $\phi = \pi/2$ boundary diminishes with decreasing K. The parameter K allows a mechanism for trading off control range over d achievable under soft switching.

Device Snubber Capacitance

The purpose of this section is to study the influence of snubber capacitance on the minimum current required at instant of turn off of any of the devices on either of the input or output bridges. It is shown here that with increasing values of snubber capacitance, the minimum current required for zero voltage switching of any of the devices increases. This further restricts the region available for soft switching on the output voltage versus output current plane.

Fig. 6(a) shows the input bridge. L is the leakage inductance of the transformer (magnetizing inductance is assumed infinite). $C1$ and $C2$ are the snubber capaci-

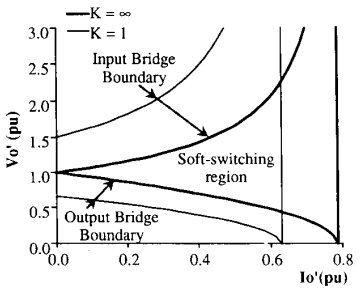

Fig. 5. Influence of transformer magnetizing inductance on the soft switching region of operation, shown on the output voltage—output current plane.

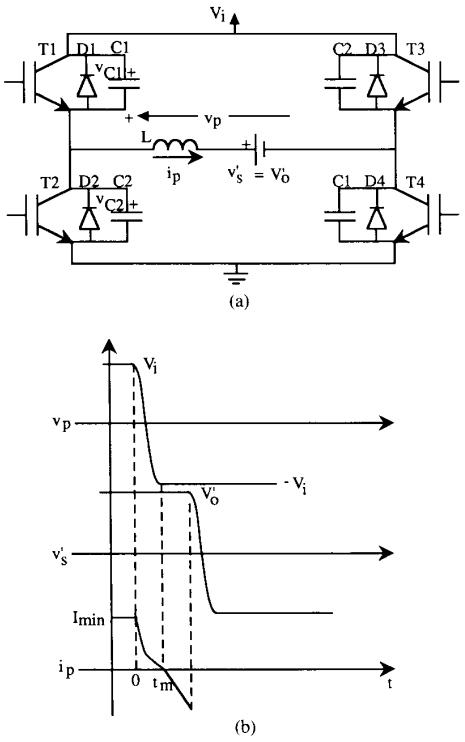

Fig. 6. (a) DAB converter with the output bridge replaced by an equivalent voltage source during turnoff of devices $T1$, $T4$ of input bridge; (b) minimum inductor current required at instant of turnoff of $T1$, $T4$ to resonate the pole voltage from $+V_i$ to $-V_i$.

tances for the input bridge devices $T1$ ($T4$) and $T2$ ($T3$). Note that $C1 = C2$. The influence of snubber capacitance on the minimum current required to flow thorugh L for zero-voltage switching on the input devices is investigated. The analysis is for the case where the input bridge is phase leading the output bridge. Moreover, even though the analysis is done for a switching event on the input bridge, the results hold for any switching event on the output bridge as well, provided the two events do not overlap (which would violate the soft-switching constraints). Let us assume that at $t = 0$, the device $T1$ ($T4$) turns off, as shown in Fig. 6(b). All other devices shown are not conducting at this time. The turn-off time of the device is considered negligible, and the value of $C1$ (or $C2$) is sufficiently large to ensure very little change in the voltage across $T1$ during its turn-off time. Once the device turns off, the current in L discharges $C2$ and charges $C1$ in a resonant manner until their respective voltages reach the opposite rails, at which point, if the current is still positive, diode $D2$ ($D3$) turn on clamping the voltage across $C2$ to zero and that of $C1$ to V_i. The current i_p through L is in the direction shown in Fig. 6(a). The output bridge is replaced by a primary-referred voltage source V_o' with the polarity required during this event. We need to find the minimum i_p at $t = 0$, which ensures that the voltage across $T1$ ($T4$) reaches the clamping value V_i when i_p reaches zero. Let $t = t_m$ be the time at which i_p just reaches zero. Hence, at t = 0

$$i_p = I_{\min}; \quad v_{C1} = 0; \quad v_{C2} = V_i$$

and at $t = t_m$

$$i_p = 0; \quad v_{C1} = V_i; \quad v_{C2} = 0.$$

During, the interval $0 \le t \le t_m$

$$i_p = 2C\frac{dv_C}{dt}. \tag{7}$$

From energy balance considerations

$$E_{(t=0)} = E_{(t=t_m)} + E_{\text{loss}} + E_{\text{delivered}}.$$

Assuming lossless circuit elements, we get

$$\frac{1}{2}LI_{\min}^2 = E_{\text{delivered}}. \tag{8}$$

Now

$$E_{\text{delivered}} = \int_0^{t_m} V_o' i_p \, dt = 2CV_o' \int_0^{t_m} v_C.$$

Zero voltage switching condition dictates that the $dv_C = V_i$ during the interval $0 \le t \le t_m$, hence

$$E_{\text{delivered}} = 2CV_o'V_i \tag{9}$$

and from (8) and (9)

$$I_{\min} = \frac{2}{Z_o}\sqrt{V_iV_o'} \qquad \text{where, } Z_o = \sqrt{\frac{L}{C}}.$$

Normalizing I_{min} with respect to $V_i/\omega L$ and defining $\omega_0 = 1/\sqrt{LC}$

$$I_{\min(pu)} = \frac{2}{\omega_n}\sqrt{d} \tag{10}$$

where

$$d = \frac{V_o'}{V_i} \qquad \omega_n = \frac{\omega_o}{\omega}$$

and ω is the switching frequency in radians per second.

Based on this analysis, the minimum output current for each load and different ω_n's can be calculated. Fig. 7

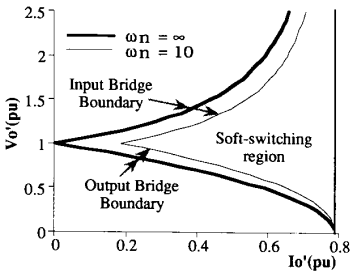

Fig. 7. Influence of device snubber capacitance on the soft-switching region of operation shown on the output voltage—output current plane. ω_n decreases as snubber capacitance increases.

shows the reduction in the soft switching region on the output voltage–output current plane with increasing snubber capacitance (decreasing ω_n). Clearly, as C is increased, switching losses decrease. However, the minimum current restricts the output voltage–output current region under soft-switching conditions. It should be noted that the decrease in VA plane due to C is compensated at least in part by the impact of the transformer magnetizing inductance. A good design must take into account all these parameters for high efficiency and wide range of control.

Control Strategies

Voltage Mode Control

Various control schemes for output voltage control can be implemented. The simplest control scheme is a voltage controller that modifies the phase shift between the primary and secondary bridges dependent on the error in the output voltage. A proportional-plus-integral controller could be used to minimize steady-state error. Limits also need to be set to ensure device soft switching.

Current Mode Control

The current command is derived from the voltage error after being processed through a proportional-plus-integral compensator. This scheme allows inherent current limiting, and the dynamics of the overall system are reduced to that of a single-order system.

Mode-Hopping Control

As seen from Fig. 3, under light- to no-load conditions, the region of soft switching is drastically reduced. This implies that in maintaining the output voltage under light loads, the converter may have to be hard switched. However, recognizing the bidirectional power flow capability of the dual active bridge converter under light load conditions, a "mode-hopping" strategy can be implemented, wherein the system is cycled sequentially between the forward and reverse power flow to maintain the desired average output voltage. This allows the converter to remain in the soft-switching region even while operating at light load.

Extended Converter Control

The DAB converter, in essence, has another topological variation. With the output bridge running as a diode bridge, the two poles of the input bridge can be phase shifted to control the amount of power flow. This mode of operation allows only unidirectional power flow and a restricted range of control. Fig. 8 shows a superposition of the output voltage versus output current characteristics, under soft switching, of the two topological modes of operation. It is seen that a wider range of control is achievable with soft switching. A significant implication of this is that the load current could be held constant even under short-circuit faults with the devices always operating under soft-switching conditions.

Experimental Results

A prototype converter was designed and fabricated for a power transfer of 50 kW, switching at 50 kHz, for an input voltage of 200 Vdc and a nominal output voltage of 1600 Vdc. The high output voltage requirement makes the use of active output bridges difficult as devices rated in the kilovolt range are limited in terms of switching speed. In addition, the high-power density needed mandates a high switching frequency. Thus, a series modular approach is necessary for realizing high power at the high-output voltages. For the specified output voltage, a cascaded connection of two active half bridges is used, as shown in Fig. 9. The two secondary side bridges are identically phase shifted from the input bridge. Fig. 10 shows the layout of the 50-kW, 50-kHz DAB converter, which has been fabricated in the laboratory.

To realize the high-power densities and minimize the electrical parasitics, multilayer planar power buses and decoupling techniques have been used. The switching devices used are insulated gate bipolar transistors (IGBT's). Multilayer ceramic capacitors (MLC's) with high rms current handling capabilities, very low effective series resistances (at the operating frequency and higher), and high-energy densities have been utilized to realize the input and output filters. The snubber capacitors are of the silver-mica type. The entire converter is water cooled.

Since the leakage inductance of the transformer is the main energy transfer element, it must be carefully controlled. Such a design objective is relatively difficult to meet in conventional transformers. A shell-type transformer with coaxial windings, details of which are reported in [2], has been fabricated to meet the above requirement. Since the majority of the leakage flux is confined to within the interwinding space, the leakage inductance can be reasonably controlled to the desired amount, and core losses due to localized saturation are virtually eliminated. Fig. 11 is a photograph of the fabricated transformer. The two litz-wire wound secondaries, each consisting of six turns, are enclosed in a three-turn primary made of rectangular copper wave guides fabricated into "U" shapes. The core consists of three pairs of PC40 Ferrite *E-E* cores. The power density of the com-

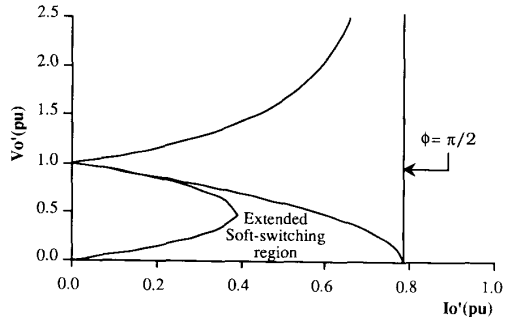

Fig. 8. Extension of soft-switching region of the DAB converter by operating the input bridge in the phase-shifted mode with the output bridge running as an uncontrolled rectifier.

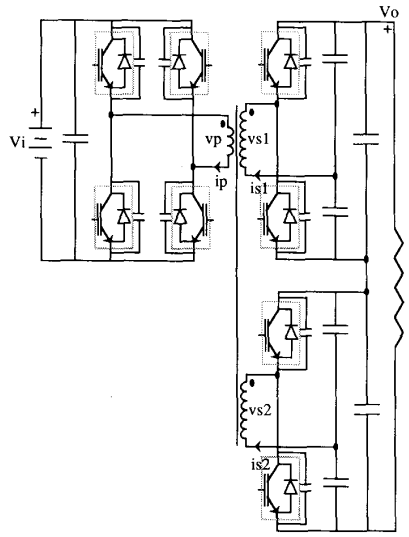

Fig. 9. Circuit schematic of high-voltage DAB converter with series-connected half bridges on the output high-voltage side.

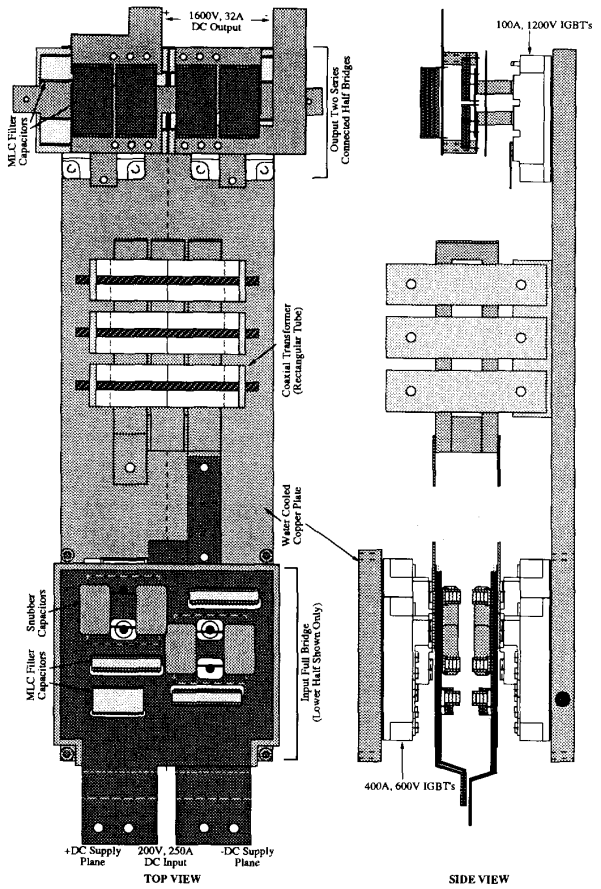

Fig. 10. Experimental layout of the 50-kW, 50-kHz DAB converter. Circuit schematic shown in Fig. 9.

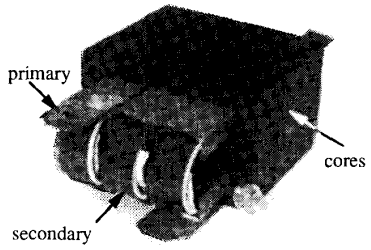

Fig. 11. Photograph of coaxial transformer rated for 50 kW and 50 kHz using rectangular tubes for the primary winding and Litz wire for the secondary winding.

pleted transformer is 0.083 kg/kW for a power transfer of 46 kW at 50 kHz. Total transformer losses have been measured as 250 W for the same power transfer, giving a projected efficiency of 99.4%. The primary-referred magnetizing inductance is 250 μH, whereas the leakage inductance has been measured as 150 nH. However, the leakage inductance (primary referred) required at the design point and rated specifications is 1.1 μH. The additional inductance was incorporated in each of the two secondary windings.

The overall weight power density of 0.24 kg/kW, a significant portion of which includes the IGBT device package weight, meets the specified target of 0.2-0.3 kg/kW. The volumetric density is in excess of 80 W/cu.in.

Forward Power Transfer

Fig. 12 shows oscillograms of the DAB converter under forward power transfer mode for a peak converter power of 48 kW at 50 kHz and $d = 1$. The overall efficiency is 87.2%, which is primarily degraded by the device package inductance and the dynamic turn-on process of the IGBT. The oscillations seen on the transformer voltages are due to resonances induced between the device package inductance (estimated as 80 nH) and the snubber capacitance. A detailed analysis reveals that the additional losses incurred due to energy trapped in the stray device inductance, diode reverse recovery, and dynamic turn-on for the test result shown in Fig. 12 are 1512 W. The projected

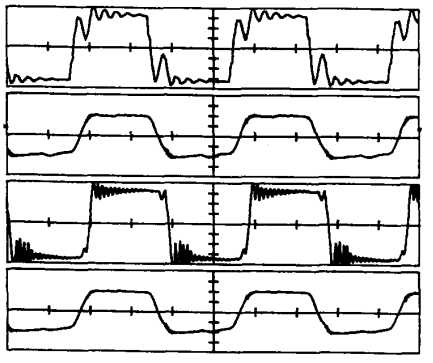

Fig. 12. Oscillograms from the experimental setup under forward power transfer at peak converter power of 48 kW, $f = 50$ kHz, $d = 1$, $V_i = 170$ Vdc, $V_o = 1288$ Vdc, $\eta = 87.2\%$. Traces from top: v_p, 50 V/div; i_{s1}, 50 A/div; v_{s2}, 100 V/div; i_{s2}, 50 A/div. Time: 5 ηs/div.

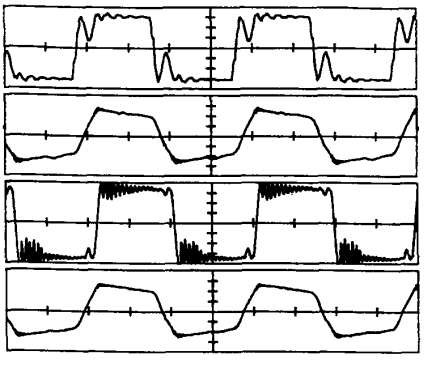

Fig. 13. Oscillograms from the experimental setup under forward power transfer at peak converter power of 49.4 kW, $f = 50$kHz, boost mode, $V_i = 161$ Vdc, $V_o = 1301$ Vdc, $\eta = 84.8\%$. Traces from top: v_p, 50 V/div; i_{s1}, 50 A/div; v_{s2}, 100 V/div; i_{s2}, 50 A/div. Time: 5 ηs/div.

efficiency in the absence of these losses is thus 90%! Similar analysis for other test results show a consistent improvement in efficiency of 3–4%. Fig. 13 shows oscillograms under boost operation.

Bidirectional Power Transfer

Under light to no-load conditions, the region of soft switching is drastically reduced. This implies that in maintaining the output voltage under light loads, the converter may have to be hard switched. However, recognizing the bidirectional power flow capability of the DAB converter, under these conditions, a "mode-hopping" strategy can be implemented, wherein the system is cycled sequentially between forward and reverse power transfer modes of operation to maintain the desired average output voltage. This allows the converter to still operate in the soft-switching region. Fig. 14 shows the converter waveforms under bidirectional power transfer, where the system is cycled 55% of the time in the forward mode and 45% in the reverse mode for a net output power of 440 W. It may be observed that the converter current adjusts from one mode to the other in half a switching cycle.

<-- Forward | Reverse -->

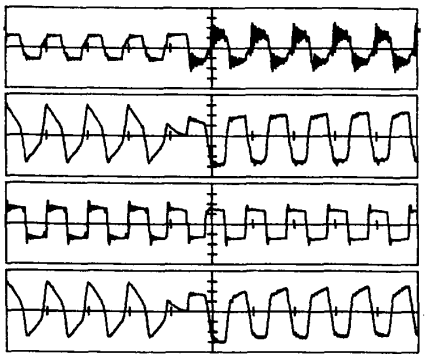

Fig. 14. Oscillograms from the experimental setup under bidirectional power transfer. Average output power = 440 W, $f = 50$ kHz, $d = 1$, $V_i = 69$ Vdc, $V_o = 551$ Vdc. Traces from top: v_p, 50 V/div; i_{s1}, 20 A/div; v_{s2}, 100 V/div; i_{s2}, 20 A/div. Time: 20 ηs/div.

Conclusions

The performance characteristics of a high-power, high-power-density dc-to-dc converter based on the single-phase dual active bridge topology are outlined. The dual active bridge converter has very attractive features in terms of low device and component stresses, small filter components, low switching losses, bidirectional power flow, buck-boost operation, low sensitivity to system parasitics, and simple first-order stable dynamics. Since the leakage inductance of the transformer is the main energy transfer element, coaxial transformer design techniques have been utilized to carefully control this parameter. Experimental results from a 50-kW, 50-Hz prototype are presented.

The most significant problem was found to be the device package. Commercially available IGBT modules are not suitable for high-density high-frequency applications because of large size and high internal inductance. Significant gains in performance and power density would be possible with improved device packages. The advent of lower forward-voltage IGBT's and new MOS-controlled thyristors would substantially further increase the efficiency of the system. To conclude, the dual active bridge converter has been shown to be a viable topology for high-power dc-to-dc converter applications in which power density constraints are important.

References

[1] R. W. DeDoncker, D. M. Divan, and M. H. Kheraluwala, "A three-phase soft-switched high power density dc-to-dc converter for high power applications," *IEEE Trans. Industry Applications*, vol. 27, no. 1, pp. 63–73, Jan./Feb. 1991.

[2] M. H. Kheraluwala, D. W. Novotny, and D. M. Divan, "Coaxially wound transformers for high-power high-frequency applications," *IEEE Trans. Power Electron.*, vol. 7, no. 1, pp. 54–62, Jan. 1992.

[3] S. Cuk and R. D. Middlebrook, *Advances in Switched-Mode Power Conversion*, vols. 1–3, 1983.

[4] O. D. Patterson, D. M. Divan, "Pseudo-resonant dc/dc converter," in *IEEE-PESC Conf. Rec.*, 1987, pp. 424–430.

[5] K. H. Liu and F. C. Lee, "Zero-voltage switching technique in dc/dc converters," in *IEEE-PESC Conf. Rec.*, 1986, pp. 284–289.

[6] K. H. Liu, R. Oruganti, and F. C. Lee, "Resonant switches—Topologies and characteristics," in *IEEE-PESC Conf. Rec.*, 1985, pp. 106–116.
[7] F. C. Schwarz and J. B. Klaassens, "A controllable 45 kW current source for dc machines," *IEEE Trans. Industry Applications*, vol. IA-15, no. 4, pp. 437–444, July/Aug. 1979.
[8] H. A. Peterson and N. Mohan, "Power supply for high power loads," U.S. Patent 4,079,305, Mar. 14, 1978.
[9] M. Ehsani, R. L. Kustom, and R. W. Boom, "A one-phase dual converter for two-quadrant power control of super conducting magnets," *IEEE Trans. Magn.*, vol. MAG-21, no. 2, pp. 1115–1118, Mar. 1985.
[10] M. H. Kheraluwala and D. M. Divan, "Design considerations for high power density dc/dc converters," in *Proc. HFPC Conf. Rec.*, May 1990, pp. 324–335.
[11] R. W. DeDoncker, D. M. Divan, and M. H. Kheraluwala, "Power conversion apparatus for dc/dc conversion using dual active bridges," U.S. Patent 5,027,264.

Mustansir H. Kheraluwala received the B. Tech. (Hons.) in electrical engineering from the Indian Institute of Technology, Kharagpur, India, and the M.S. and Ph.D. degrees in electrical engineering from the University of Wisconsin, Madison, in 1984, 1987, and 1991, respectively.

He is presently working with the Power Systems Technologies Group at the General Electric Company, Corporate Research and Development, Schenectady NY. His research interests are in the area of power electronics and electrical machines.

Dr. Kheraluwala is a member of the Power Electronics Society of the IEEE.

Randal W. Gascoigne (M'90) received the B.S.E.E. degree from the University of Wisconsin-Madison in 1982.

A native of Wisconsin, he specialized in analog and integrated electronics while at the University, and after graduating, he found employment at the University engineering custom instrumentation and controls for a wide variety of applications. In 1987, he joined the staff of WEMPEC to serve as the lab manager and to provide technical assistance. Since then, he has co-authored several technical papers and helped direct the rapid growth of the WEMPEC lab facilities. He finds considerable enjoyment in applying power electronics and new technology in novel ways.

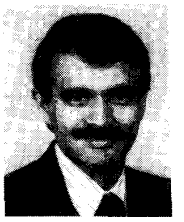

Deepakraj M. Divan (S'78–M'78–S'82–M'83) received the B.Tech. degree in electrical engineering from the Indian Institute of Technology, Kanpur, India, and the M.Sc. and Ph.D. degrees in electrical engineering from the University of Calgary, Calgary, Canada, in 1975, 1979, and 1983, respectively.

He worked for two years as a Development Engineer with Philips India Ltd. In 1979, he started his own concern in Pune, India, providing product development and manufacturing services in the power electronics and instrumentation areas. In 1983, he joined the Department of Electrical Engineering at the University of Alberta as an Assistant Professor. Since 1985, he has been with the Department of Electrical and Computer Engineering at the University of Wisconsin, Madison, where he is presently an Associate Professor. He is also an Associate Director of the Wisconsin Electric Machines and Power Electronics Consortium (WEMPEC). His primary areas of interest are in power electronic converter circuits and control techniques. He has over 25 papers in the area as well as many patents.

Dr. Divan was a recipient of the Killam Scholarship and a co-recipient of the 1988 Third Prize Paper Award in the Power Semiconductor Committee and the 1983 Third Prize Paper Award of the Static Power Converter Committee of the IEEE Industry Applications Society. He is also a consultant for various industrial concerns. He was the Program Chairman for the 1988 and 1989 Static Power Converter Committee of the IEEE-IAS, Program Chairman for PESC 91, and a Treasurer for PESC 89. He is also a Chairman of the Education Committee in the IEEE Power Electronics Society.

Eric D. Baumann received the B.E.E. degree from Cleveland State University, Cleveland, OH, and the M.B.A. degree from Baldwin Wallace College, Berea, OH in 1983 and 1990, respectively.

Since 1985, he has been with the Power Technology Division of the NASA Lewis Research Center in Cleveland, OH. During the past year, he has been guiding development work in the areas of ultralightweight, megawatt level power converters and high-temperature electronics for space applications.